Air Distribution in Rooms, (ROOMVENT 2000)
Editor: H.B. Awbi

EXPERIMENTAL INVESTIGATION OF A SOLAR CHIMNEY NATURAL VENTILATION SYSTEM

S. Spencer[1], Z.D. Chen[2], Y. Li[2] and F. Haghighat[1]

[1] Department of Building, Civil and Environmental Engineering
Concordia University, Canada
[2] Thermal and Fluids Engineering, CSIRO Building, Construction and Engineering
PO Box 56, Highett, Victoria 3190, Australia

ABSTRACT

Natural ventilation driven by a solar chimney attached to a single-room building is investigated experimentally with a small-scale model using a recently developed fine bubble technique. Parameters studied in the experiments are the cavity width of the solar chimney, the solar radiation intensity, the height of the solar chimney, the room inlet area and the solar chimney inlet area. Results showed that for given building geometry and inlet areas, there is an optimum cavity width at which a maximum ventilation flow rate can be achieved. This optimum cavity width, which is independent of the solar radiation intensity, was found to be dependent on the chimney height, the size of the room inlet and the size of the solar chimney inlet. Comparisons between the measured ventilation flow rate and predictions by a simple theoretical analysis presented in this paper suggested that theoretical models, which assume uniform temperature distribution across the chimney width, may overpredict the chimney performance at some situations and should be used with care.

KEYWORDS

Solar chimney, natural ventilation, experimental modelling.

INTRODUCTION

Due to increasing awareness of greenhouse gas emission and the need for effective, cost-efficient and ecologically sound building ventilation, the past two decades have seen a number of investigations to better understand ventilation in solar chimneys. Bouchair (1994) carried out an experimental investigation on a full-scale solar chimney model system. It was found that there was an optimum chimney width, occurring at about one-tenth of the chimney height, at which a maximum ventilation flow rate can be achieved. Reduced airflow rate after this optimum width was caused by the reversed flow in through the centre of the chimney outlet. Barozzi *et al.* (1992) also carried out an experimental study of a building using a 1:12 solar chimney model for cooling ventilation, and the experimental results were used to validate their two-dimensional CFD simulations. Bansal *et al.* (1993, 1994)

developed a steady-state analysis for solar chimneys. Uniform temperature distribution across the chimney width is assumed and there are no experimental validations for their theoretical analysis. In this work, experiments were carried out on the performance of a solar chimney system with a constant solar radiation incident on a single chimney wall. The effect of the chimney width and height, the solar radiation intensity, and the inlet geometry into the chimney and into the room are investigated. Experimental results are compared with a simple theoretical analysis.

THEORY

Assuming a linear temperature distribution along the solar chimney height and a uniform temperature distribution across the chimney width, it can be shown that the ventilation flow rate, Q, can be obtained by the following equation:

$$Q = A_e^{\frac{2}{3}} (BH)^{\frac{1}{3}} \tag{1}$$

where B_h is the buoyancy flux per unit height ($B_h = B/H$), B is the buoyancy flux (m^4/s^3) and H is the height of the chimney (m). A_e is the effective opening area of the system, and since the cross-sectional area of the chimney is equal to the chimney outlet area, we have:

$$A_e = \left[\frac{1}{(c_{ri} A_{ri})^2} + \frac{1}{(c_{ci} A_{ci})^2} + \left(\frac{1 + K_f c_{co}^2}{c_{co}^2} \right) \frac{1}{A_{co}^2} \right]^{-1/2} \tag{2}$$

here, c is the discharge coefficient for the room inlet (ri), the chimney inlet (ci), the chimney outlet (co) and in the chimney (sc). The loss coefficient of the chimney channel, K_f, and the discharge coefficients, c, are taken from duct design data (ASHRAE 1989) and A is the cross-sectional area (m^2).

EXPERIMENTAL

Experiments were performed in a large glass tank containing an aqueous saline solution of 4 wt%. Fine hydrogen bubbles were generated by electrolysis of saline water using a cathode–anode circuit and were used to simulate buoyancy forces in the chimney produced by temperature differences. Details of the fine-bubble experimental system can be found in Chen *et al.* (1999).

Figure 1 shows the 0.2 m (wide) × 0.1 m (deep) × 0.2m (high) perspex building model with a chimney attached. The depth (0.1 m) and height (0.2 m) of the solar chimney are fixed, while its width is adjustable. In order to investigate the effect of chimney height, a 200 mm extension to the chimney channel is attached on top of the original chimney, giving a total height of 400 mm. Buoyancy forces in the chimney are provided by fine hydrogen bubbles produced by a copper wire grid cathode attached to the right side inner wall of the chimney (refer to Figure 1). The flow velocity was measured by a particle tracking method using a video camera. The total buoyancy flux, which represents the strength of a buoyancy source, was evaluated as $B = gQ_g(\rho_l - \rho_g)/\rho_l$. Here, ρ_g and ρ_l are the densities of hydrogen gas and the salt-water solution respectively, and Q_g is the hydrogen gas flow rate.

In this work, experiments were performed at a chimney width ranging from 5 to 30 mm for the 200mm chimney, and from 10 to 50 mm for the 400 mm chimney. The effect of chimney width, buoyancy flux strength, chimney height and inlet area on the ventilation flow rate were investigated. The opening

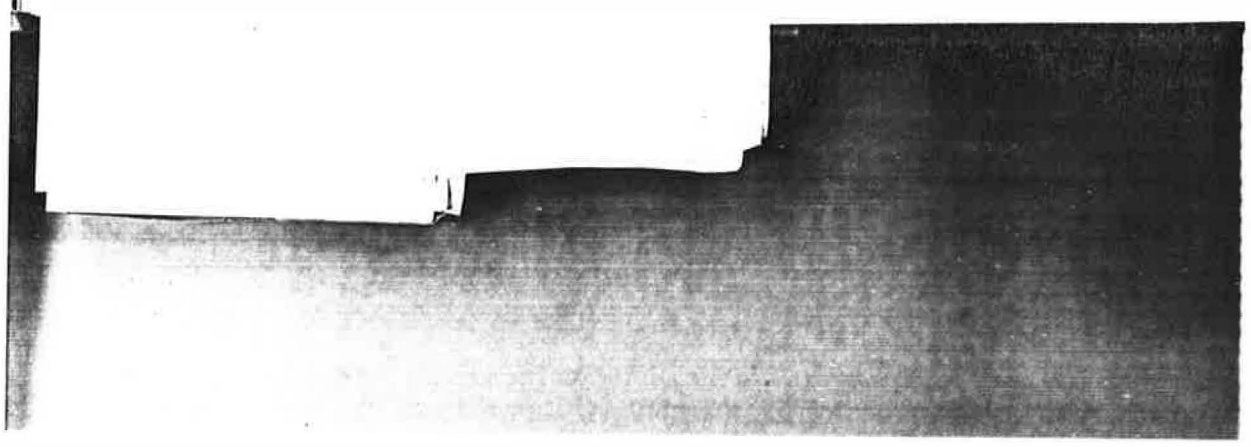

modes are categorised according to the inlet areas to the room and to the chimney. They are defined in Table 1.

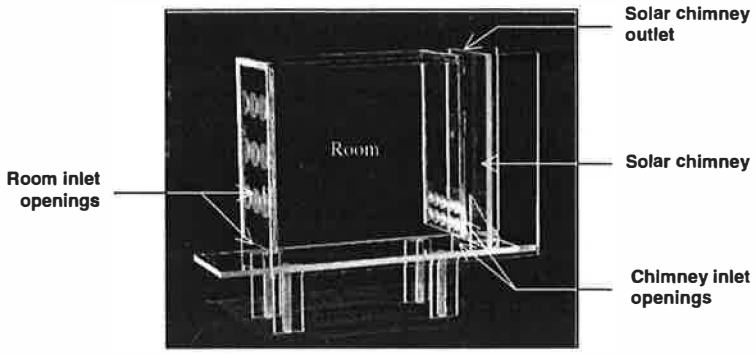

Figure 1: Solar chimney model (note that the two top rows of openings into the room are not used in the experiments)

TABLE 1
DEFINITION OF OPENING MODES

Mode	Room inlet		Chimney inlet	
	Opening geometry	Area (mm^2)	Opening geometry	Area (mm^2)
I	Rectangular	1500	Rectangular	1500
II	Rectangular & circular	3000	Rectangular	1500
III	Rectangular	1500	Rectangular & circular	3000
IV	Rectangular & circular	3000	Rectangular & circular	3000

RESULTS AND DISCUSSION

Figure 2 shows the experimental results for mode I with buoyancy fluxes of 122, 244, 367 and 489 cm^4/s^3, respectively. Similar to Bouchair's (1994) results, it can be seen that there is an optimum chimney width (around 12 mm) at which the chimney provides a maximum ventilation rate. The reduction of flow rate at chimney widths larger than the optimum was observed to be associated to the reversed flow at the chimney outlet. As shown in Figure 2, increasing the buoyancy flux in the chimney increases the flow rate through the system. However, the optimum chimney width is independent of the strength of the buoyancy flux. From Bouchair's (1994) experimental results, it was also found that increasing the solar radiation intensity has little effect on the optimum chimney width, although his experiments were carried out using a full-scale solar chimney model with constant temperatures on both chimney walls.

Figure 3 shows the experimental ventilation flow rate obtained for the four opening modes with a constant buoyancy flux of 367 cm^4/s^3. In general, the larger the inlet area the larger the flow rate. It can also be noted that there is a shift in the optimum chimney width, it becoming significantly larger for

modes III and IV at around 16–18 mm. For mode II the optimum width is about the same as that for mode I, occurring at 10–14 mm. It can also be seen that a much higher ventilation flow rate can be achieved with modes III and IV. With larger inlets to the chimney, i.e. modes III and IV, increased mixing of bubbles in the chimney channel was observed. Fluid entering the chimney inlet impinges on the chimney wall and disperses the bubble plume, probably caused by a substantial increase in flow velocity, compared to the smaller chimney inlet, because of the decreased flow resistance with the larger inlet area. This suggests that the entering fluid is, at least locally, destroying the 'thermal' boundary layer along the chimney wall. Consequently, the 'temperature' (represented by bubble concentration in this work) distribution becomes more uniform in the region close to the chimney inlet than it does for the smaller inlet openings of modes I and II. Figure 4 illustrates the possible temperature distributions for the small and large chimney inlets. With a more uniform temperature distribution, a high ventilation flow rate may be achieved due to higher stack pressure.

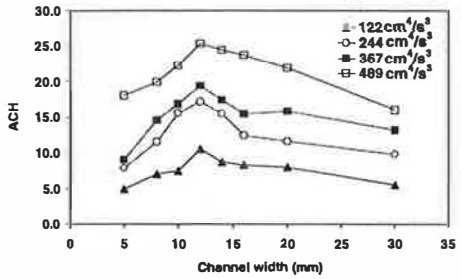

Figure 2: The effect of chimney width on ventilation flow rate for the 200 mm height chimney (ACH is the air changes per hour)

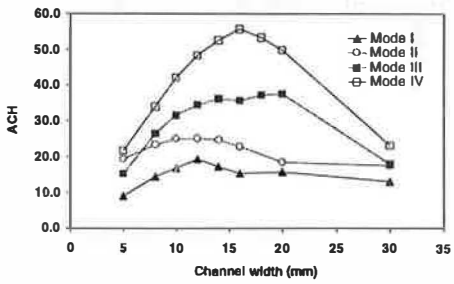

Figure 3: The effect of opening mode on ventilation flow rate for the 200 mm height chimney at a buoyancy flux of 367 cm^4/s^3

Tests were also performed for the 400 mm high chimney. The tests were carried out for a fixed buoyancy flux of 489 cm^4/s^3 for opening mode I and the results are shown in Figure 5 along with the experimental results for the same buoyancy flux and opening mode for the 200 mm high chimney. It can be seen from Figure 5 that the optimum chimney width for the 400 mm chimney is almost twice that for the 200 mm chimney.

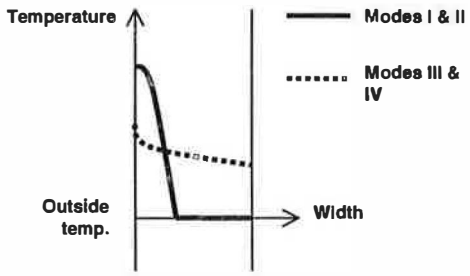

Figure 4: Possible temperature distributions in the chimney channel

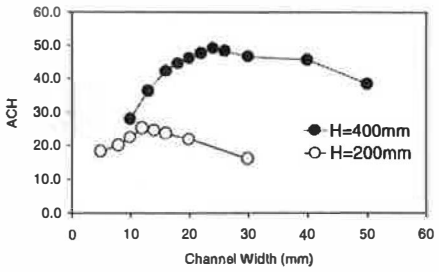

Figure 5: Influence of chimney height for mode I and 489 cm^4/s^3

Figures 6(a)–6(d) show the comparisons between the theoretical predictions (Eq. 1) and the experimental ventilation flow rate. It is seen that the theoretical predictions generally overpredict the ventilation flow rate, especially for modes I and II. At the same time, reasonably good agreement was obtained for modes III and IV when the chimney width is smaller than the optimum width. The

discrepancy between the predictions and the experimental data might be caused by the following factors. (1) In the analysis, a uniform temperature distribution across the chimney width is assumed. However, in reality, the temperature distribution looks more like that shown in Figure 4. The uneven temperature distribution across the chimney width results in lower stack pressure and ventilation flow rates compared with theoretical predictions. As shown in Figure 4, this effect may be significant for modes I and II,. Consequently, overprediction by the simple analysis is expected. While for modes III and IV, increased mixing of the bubbles in the chimney channel was observed. The more even temperature distribution across the chimney width may result in the better agreement between the experimental results and the theoretical predictions for modes III and IV, as shown in Figure 6(c) and 6(d). (2) The uncertainty of the discharge coefficient values used may cause errors in the theoretical predictions. (3) For channel widths larger than the optimum, the backflow in the outlet significantly reduces the ventilation flow rate. However, the simple analysis does not incorporate the backflow effect.

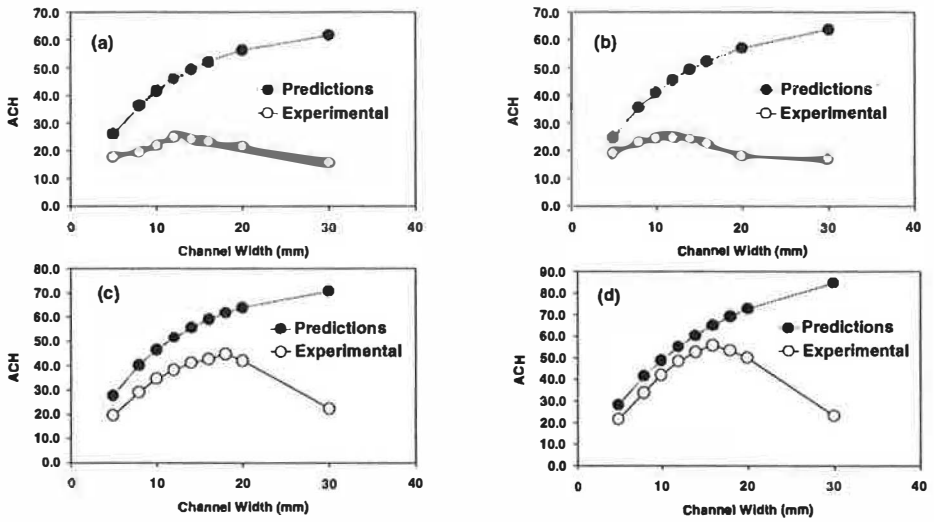

Figure 6: Comparisons between the theoretical predictions and the experimental results for 200 mm chimney: (a) mode I, B = 489 cm^4/s^3; (b) mode II, B = 367 cm^4/s^3; (c) mode III, B = 367 cm^4/s^3; and (d) mode IV, B = 367 cm^4/s^3.

SIMILARITY AND SCALE-UP CRITERIA

Due to the page limitation, only a brief discussion of the similarity analysis will be presented here. For a detailed similarity analysis, please refer to Chen *et al* (1999). For building ventilation driven by natural convection, dynamic similarity between a model and its prototype requires two dimensionless parameters to be identical in the two systems, i.e. the Rayleigh number ($Ra = BH^2/(\nu D^2)$, where D is the thermal or mass diffusivity and ν the viscosity of the fluid) and the Prandtl number (or the Schmidt number for natural convection driven by concentration differences). However, for turbulence dominated flows with sufficiently large Rayleigh numbers, the requirements for the Rayleigh number and the Prandtl number (or the Schmidt number) can be removed and the resulting flows in a model are similar to those in its corresponding prototype (Etheridge and Sanderberg, 1996). Similarity between a model and its corresponding prototype ensures that dimensionless parameters for the model should be equal to their counterparts for the prototype. Consequently, we have:

$$\left(\frac{B_{PT}H_M^4}{B_M H_{PT}^4}\right)=\left(\frac{\theta_M}{\theta_{PT}}\right)^3 \tag{3}$$

where θ is the characteristic time scale, PT the prototype and M the model. For a prototype and its related model, B_{PT}, B_M, H_{PT} and H_M are all known parameters. So, θ_M/θ_{PT} can be obtained. Then, all the other properties for the full scale, such as velocity u, the temperature difference and the volume flux through openings Q, can be obtained by the following relations:

$$\frac{\beta\Delta T}{\Delta\varphi}=\left(\frac{H_{PT}}{H_M}\right)\left(\frac{\theta_M}{\theta_{PT}}\right)^2 \tag{4}$$

$$\frac{u_{PT}}{u_M}=\left(\frac{H_{PT}}{H_M}\right)\left(\frac{\theta_M}{\theta_{PT}}\right) \tag{5}$$

and

$$\frac{Q_{PT}}{Q_M}=\left(\frac{H_{PT}}{H_M}\right)^3\left(\frac{\theta_M}{\theta_{PT}}\right) \tag{6}$$

where φ is the gas volume fraction in the liquid, β the thermal expansion coefficient of air.

CONCLUSION

Experimental investigations were carried out for a solar chimney system using a small-scale experimental model. The existence of an optimum chimney width, at which a maximum ventilation flow rate can be achieved, is confirmed in this work. The optimum chimney width is independent of source strength, but becomes larger for larger chimney inlets. The optimum chimney width increases proportionally with the chimney height in the experimental range covered in this work. Comparisons between the measured ventilation flow rate and predictions by a simple theoretical analysis suggested that theoretical models, which assume uniform temperature distribution across the chimney width, may overpredict chimney performance in certain situations and should be used with care.

REFERENCES

ASHRAE (1989). *ASHRAE Handbook of Fundamentals*, American Society of Heating Ventilation and Air-conditioning Engineers Inc., Atlanta, GA.

Bansal N. K., Mathur R. & Bhandari M. S. (1993). Solar Chimney for Enhanced Stack Ventilation. *Building & Environment* **28:3**, 373–377.

Bansal N. K., Mathur R. & Bhandari M. S. (1994). A Study of a Solar Chimney Assisted Wind Tower System for Natural Ventilation in Buildings. *Building & Environment* **29:4**, 495–500.

Barozzi G. S., Imbabi M. S. E., Nobile E. & Sousa A. C. M. (1992). Physical and Numerical Modelling of a Solar Chimney-based Ventilation System for Buildings. *Building & Environment* **27:4**, 433–445.

Bouchair A. (1994). Solar Chimney for Promoting Cooling Ventilation in Southern Algeria. *Building Serv. Eng. Res. Technol.* **15:2**, 81–93.

Chen Z. D., Li Y. & Mahoney J. (in press). Experimental Modelling of Buoyancy-driven Flows in Buildings Using a Fine-bubble Technique. *Building & Environment.*

Etheridge, D.W. and Sanderberg, M., *Building ventilation: theory and measurement*, John Wiley & Sons Ltd, 1996, pp. 206-209, 649–667.